Figure S1, related to Figure 1

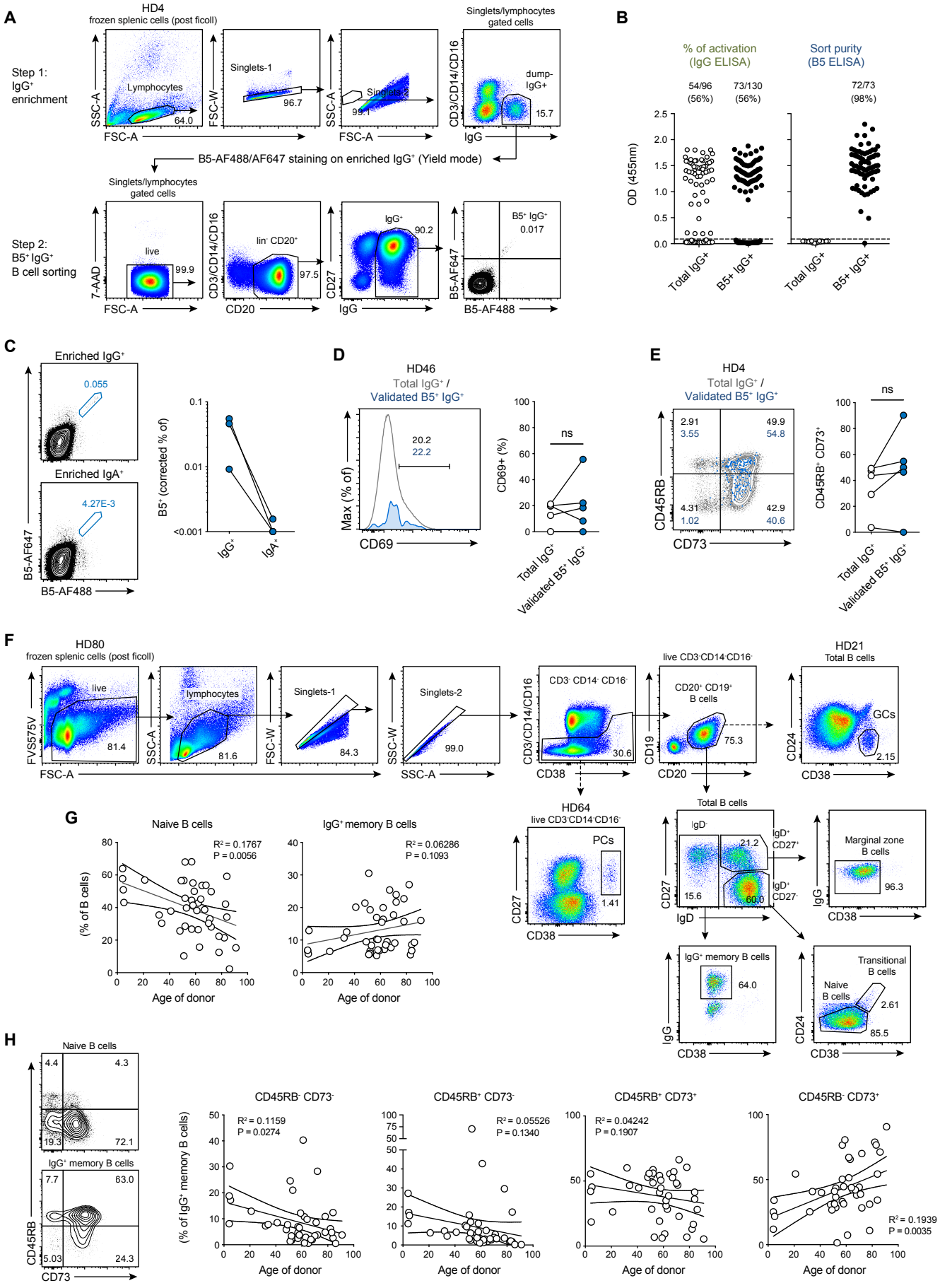

Figure S1. Flow cytometry-based characterization of long-lived splenic vaccinia-specific and total MBC populations. Related to Figure 1.

(A) Gating strategy for the two-step sorting scheme used to isolate vaccinia B5-specific IgG^+ MBCs from the spleen of organ donors. Lymphocytes were first gated based on morphology, before exclusion of doublets and enrichment of $IgG^+CD3^-CD14^-CD16^-$ cells. Enriched IgG^+ were further tightly gated based on morphology, before exclusion of doublets, dead cells and residual CD3/CD14 cells. The B5-$AF488^+$ B5-$AF647^+$ upper right quadrant was then single-cell sorted from gated IgG^+CD20^+ switched MBCs. **(B)** IgG ELISA values on all sorted wells (left) and B5 ELISA values on IgG^+ wells (right) from a representative sort (Optical Density at 450nm (OD)). Cut-offs are set at 0.1nm. **(C)** Representative dot-plots of B5-staining (Left) and graph showing the corrected frequencies of B5-specific MBCs in enriched IgG^+ or IgA^+ live $CD20^+$ splenic B cells (Right, *n* = 3 donors). **(D)** Representative overlayed histograms of CD69 staining (Left) and graph showing the frequencies of $CD69^+$ in culture-validated $B5^+IgG^+$ or total IgG^+ live $CD20^+$ splenic B cells (Right, *n* = 5 donors). **(E)** Representative overlayed dot-plots of CD73 and CD45RB staining (Left) and graph showing the frequencies of $CD73^+CD45RB^+$ in culture-validated $B5^+IgG^+$ or total IgG^+ live $CD20^+$ splenic B cells (Right, *n* = 4 donors). **(F)** Flow cytometry gating strategy for the analysis of splenic B cell populations. Dead cells were first excluded prior to lymphocyte gating based on morphology and exclusion of doublets. PCs and B cells were further gated as respectively $CD27^+CD38^{hi}$ and $CD20^+CD19^+$ cells in gated $CD38^{+/-}CD3^-CD14^-CD16^-$ lymphocytes. B cells were further subdivided as $CD24^-CD38^{int}$ GCs (GC) B cells, $IgD^-CD27^-CD24^-CD38^-$ naive B cells, $IgD^-CD27^-CD24^{int}CD38^{int}$ transitional B cells, $IgD^+CD27^+IgG^-CD38^-$ marginal zone B cells (MZBs) and $IgD^-IgG^+CD38^-$ switched MBCs. One representative donor is shown for major splenic B cell population, but donors with clear populations of GC B cells or PCs are shown for these specific populations (see also Figure S3D). **(G)** Frequencies of naive (left) and IgG^+ MBCs (right) in live splenic B cells plotted against donor's age (*n* = 42 donors). **(H)** Representative dot plots of CD73 and CD45RB staining in naive (top left and IgG^+ MBCs (bottom left) live splenic B cells and graphs showing the frequencies of $CD45RB^-CD73^-$ (second from the left), $CD45RB^+CD73^-$ (middle), $CD45RB^+CD73^+$ (middle right) and $CD45RB^-CD73^+$ (far right) in IgG^+ MBCs plotted against donor's age (*n* = 42 donors). (D-E) Wilcoxon matched-pairs signed rank test (ns = non-significant). (G-H) Linear regression and 95% confidence intervals are shown.

Figure S2, related to Figure 2

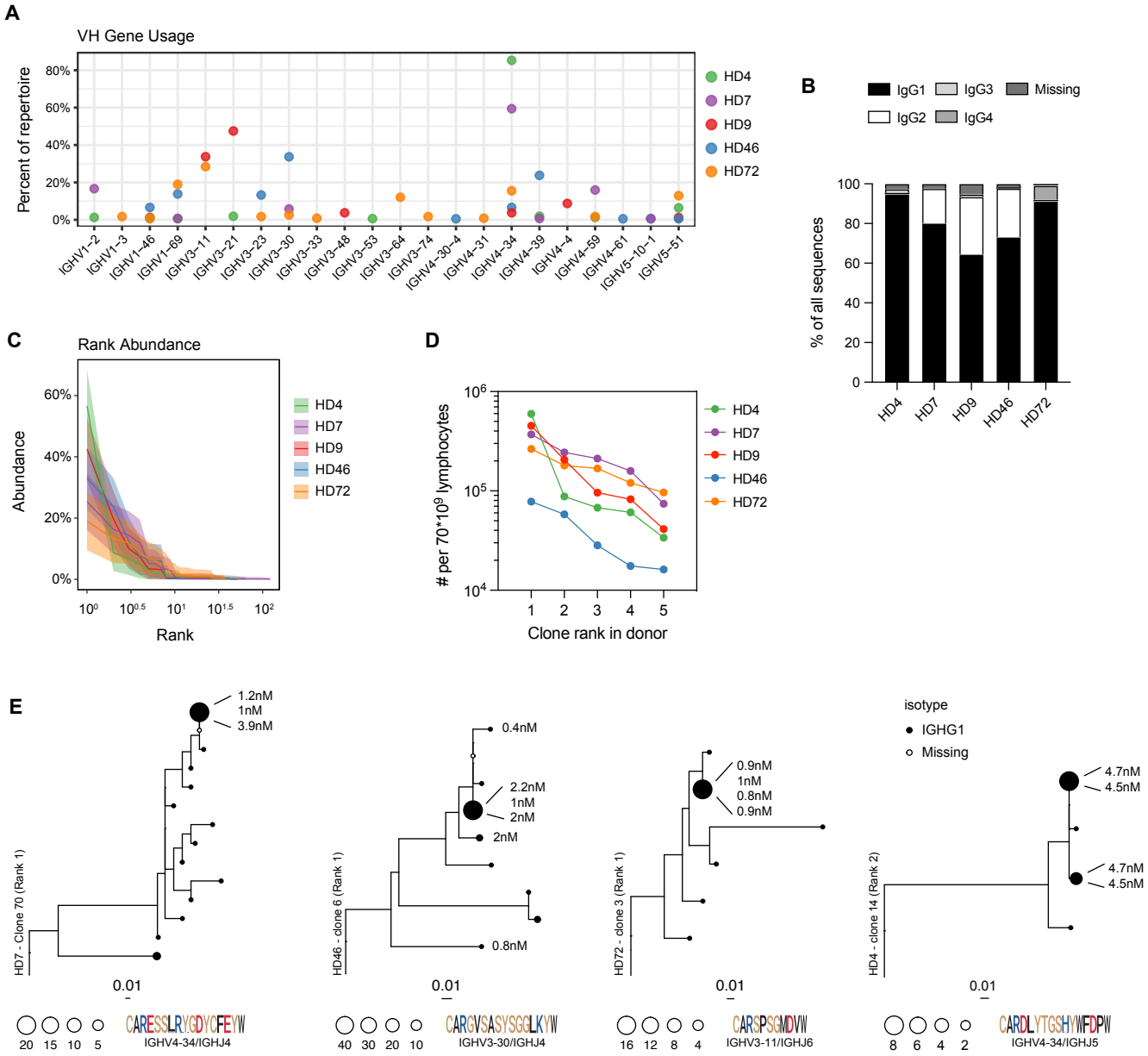

Figure S2. VH genes usage, isotypes, diversity and clone size of the B5-specific long-lived MBC repertoire. Related to Figure 2.

(A-D) Plots showing the frequency of individual VH gene usage (A), the frequency of individual isotype usage (B), the frequency (C) and estimated size (D) of individual clones ranked based on clone size for the B5-specific IgG^+ MBC repertoire of the five sequenced donors. **(E)** Representative lineage trees for B5-specific IgG^+ MBC clones. Dot size represents the number of sorted cells sorted bearing V_H sequences with identical somatic mutations. Dot color represents the identified isotype. Donor, clone number and rank are labeled on the left side of each tree. Affinities from tested supernatants are displayed on the right side of each tree in front of related sequence nodes. Sequence logo representing all CDR3s inside that clone, as well as V and J calls, is added on the bottom right.

Figure S3, related to Figure 3

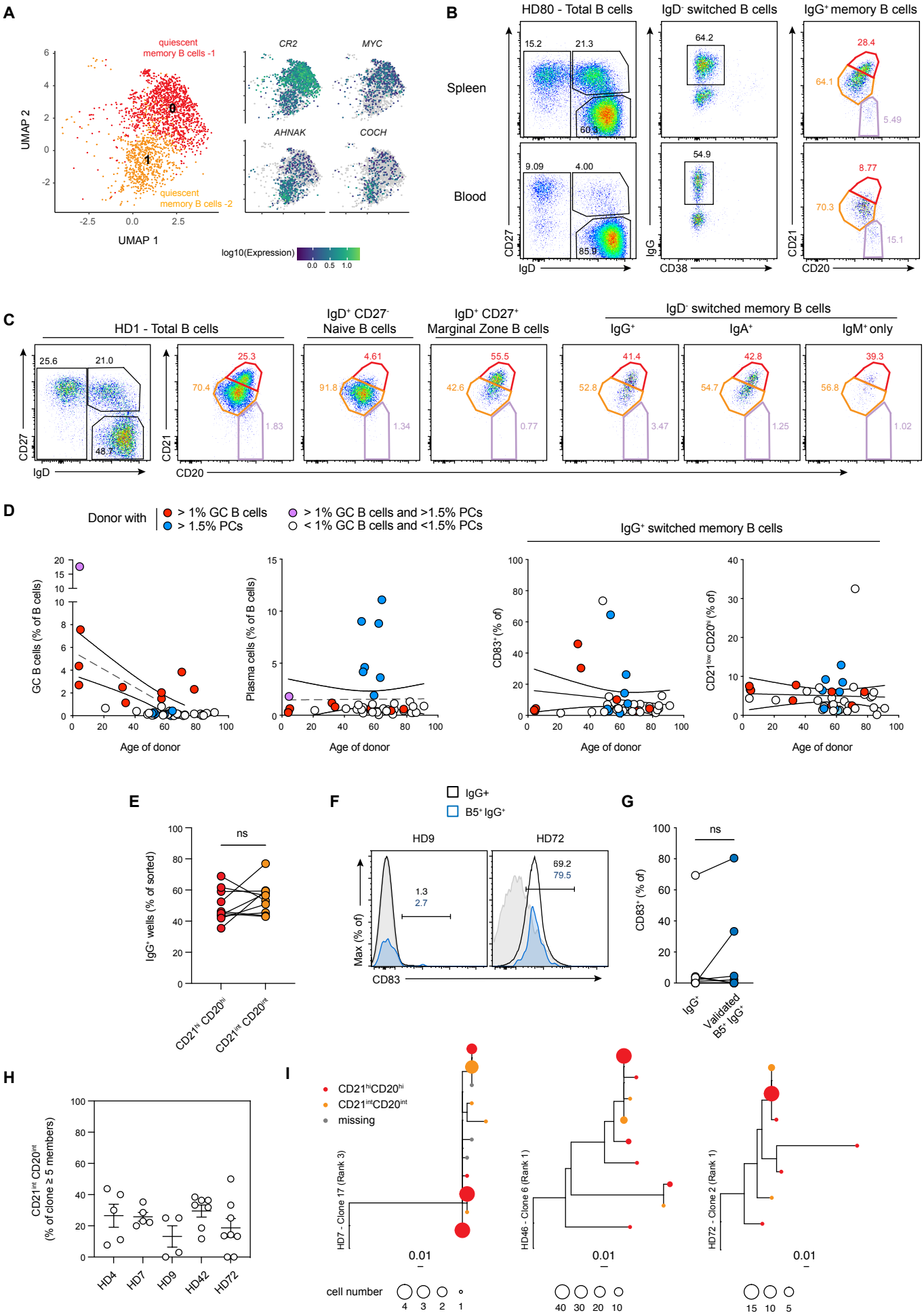

Figure S3. Identification of CD21^{hi}CD20^{hi}, CD21^{int} CD20^{int} and CD83^{+} B cell subsets and clonal relationships between B5-specific CD21^{hi}CD20^{hi} and CD21^{int}CD20^{int} IgG^{+} MBC subsets. Related to Figure 3.

(A) UMAP and clustering of quiescent MBCs identified in our scRNA-seq (left) and feature plots for CR2 (CD21), MYC, AHNAK and COCH for cells in these two clusters (right). **(B)** Representative dot plots for CD27 and IgD staining in gated CD3^{-}CD14^{-}CD16^{-}CD20^{+} B cells (left), IgG and CD38 staining in gated CD3^{-}CD14^{-}CD16^{-}CD20^{+}IgD^{-} switched MBCs (middle) and CD21 and CD20 staining in gated CD3^{-}CD14^{-}CD16^{-}CD20^{+}IgD^{-}CD38^{-} IgG^{+} circulating (PBMCs) or splenic MBCs (right). **(C)** Representative dot plots for CD21 and CD20 staining in gated CD3^{-}CD14^{-}CD16^{-}CD20^{+} B cells and indicated splenic B cell subsets. **(D)** Graphs showing the frequencies of GC B cells (far left) and PCs (middle left) in total splenic B cells and the frequencies of CD83^{+} (middle right) and CD21^{lo}CD20^{hi} (far right) in splenic IgG^{+} MBCs plotted against donor's age (n = 42 donors). Linear regression and 95% confidence intervals are shown. Donors with >1% GC B cells, >1.5% PCs or both are highlighted in red, blue and purple respectively. **(E)** Frequencies of IgG^{+} wells after 18-21 days co-culture with B21 feeder cells and single cell sorted CD21^{hi}CD20^{hi} and CD21^{int}CD20^{int} IgG^{+} MBCs, showing that both populations are similarly activated in our assay. **(F-G)** Overlayed histograms of CD83 staining for two representative donors (F) and graph showing the frequencies of CD83^{+} in culture-validated B5^{+}IgG^{+} or total IgG^{+} live CD20^{+} splenic B cells (G, n = 5 donors). **(H)** Frequencies of sequences isolated from CD21^{int}CD20^{int} for each individual B5-specific IgG^{+} MBC clone of size ≥ 5. **(I)** Representative lineage trees for B5-specific IgG^{+} MBC clones. Dot size represents the number of sorted cells sorted bearing V_H sequences with identical somatic mutations. Dot color represents the index-sorting phenotype of sorted cells (red = CD21^{hi}CD20^{hi}, orange = CD21^{int}CD20^{int}, grey = missing index sorting information). Donor, clone number and rank are labeled on the left side of each tree. (E, G) Wilcoxon matched-pairs signed rank test (ns = non-significant).

Figure S4, related to Figure 4

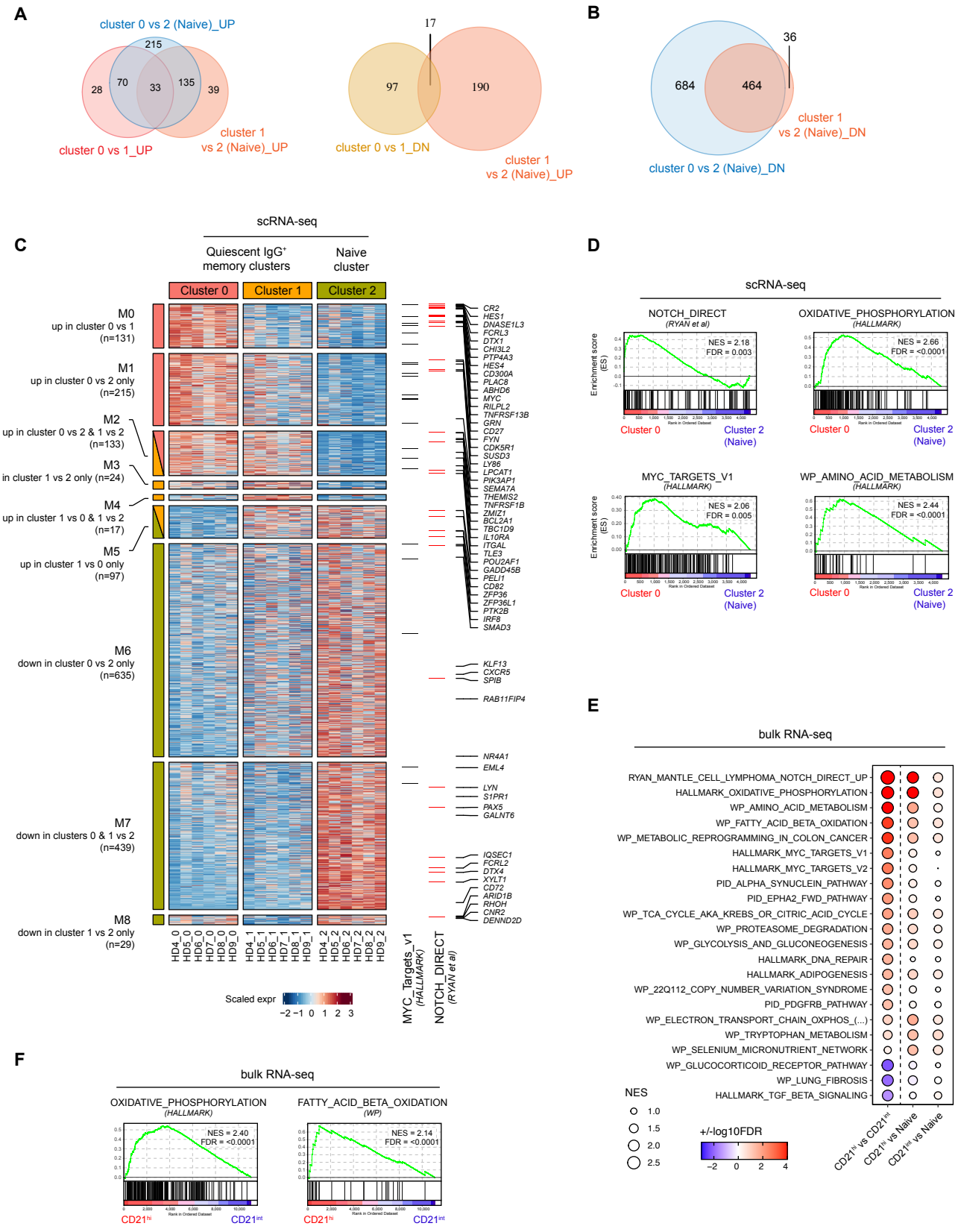

Figure S4. Transcriptional signature of CD21^{int} and CD21^{hi} IgG^{+} splenic MBCs. Related to Figure 4.

(A-B) Venn diagrams of differentially expressed gene signatures in various comparisons between cluster 0, cluster 1 and cluster 2 cells from our scRNA-seq dataset (cluster 0 versus 2 (Naive)_UP: significantly upregulated in cluster 0 versus cluster 2 cells; cluster 0 versus 1 _DN: significantly downregulated in cluster 0 versus cluster 1 cells). **(C)** Heatmap showing scRNA-seq expression data for all donors from which splenic naive, total memory and vaccinia-specific MBCs were sorted and for all genes significantly upregulated or downregulated in one of the three comparisons: cluster 0 versus 1, cluster 0 versus 2 and cluster 1 versus 2. Data are displayed as row-scaled pseudobulk expression averaging all cells from a given cluster and donor. Genes are further clustered based on the comparison(s) in which they come out as significant and ordered based on the fold change in expression between cluster 0 and 1. Group labels, conditions of inclusion and number of included genes are indicated on the left side of the heatmap. Genes belonging to the HALLMARK_MYC_Targets_v1 (black lines) and RYAN_NOTCH_DIRECT genesets (red lines and gene labels, (Ryan et al., 2017) are further highlighted on the right side of the heatmap. **(D)** Enrichment plots for indicated genesets in the comparison of cluster 0 (CD21^{hi} IgG^{+} MBCs) versus cluster 2 (naive B cells) in our scRNA-seq dataset. **(E)** Plot showing the preranked Geneset Enrichment Analysis (GSEA) results for all three comparisons performed on our bulk RNA-seq dataset between CD21^{hi} or CD21^{int} IgG^{+} MBCs and naive B cells. Dot size represents the Normalized Enrichment Score (NES). Dot color represents the sign of the log fold change * log10(False Discovery Rate value (FDR)). Only genesets with a NES > 1.5 and FDR < 0.01 in one of the 3 comparisons are shown. Top differentially expressed gene upregulated in cluster 0 versus cluster 1 in the leading-edge subset of each geneset are further highlighted on the right side of the plot. **(F)** Enrichment plots for indicated genesets in the comparison of CD21^{hi} versus CD21^{int} IgG^{+} MBCs. See also Table S3.

Figure S5, related to Figure 4

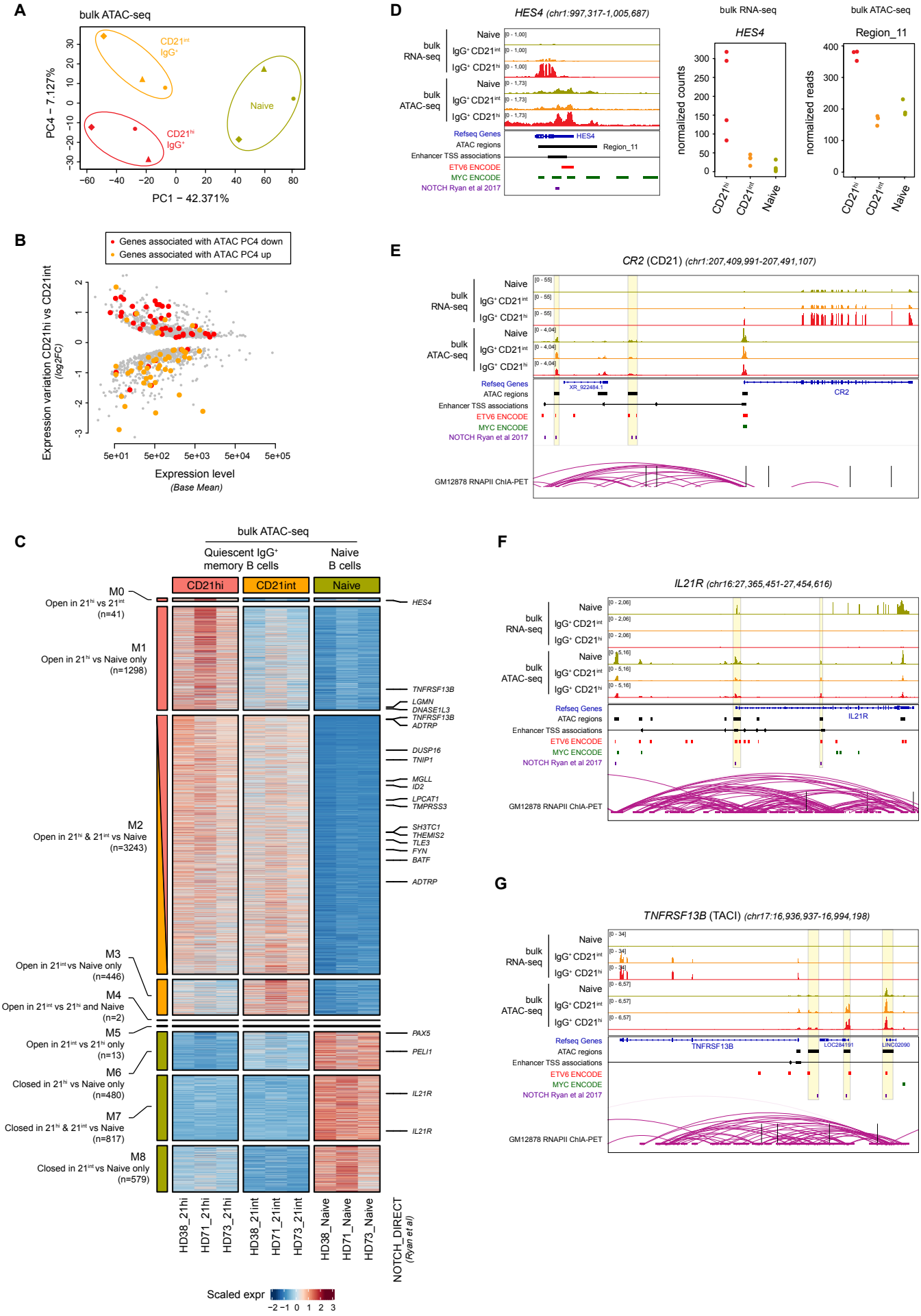

Figure S5. Differential chromatin accessibility for NOTCH target genes in CD21^{int} and CD21^{hi} IgG^{+} splenic MBCs as compared to naive B cells. Related to Figure 4.

(A) PCA analysis of bulk ATAC-seq data for paired naive, CD21^{int} and CD21^{hi} IgG^{+} samples isolated from the spleen of organ donors (*n* = 3). **(B)** Plot showing the log2 of the fold change (Log2FC)) in RNA expression for differentially expressed genes in the comparison of sorted CD21^{hi}CD20^{hi} and CD21^{int}CD20^{int} IgG^{+} MBCs. Genes associated with the aPC4 of the bulk ATAC-seq PCA analysis reported in (A) are highlighted. **(C)** Heatmap showing row-scaled bulk ATAC-seq peak accessibility data for all regions significantly differentially accessible in one of the three comparisons between sorted naïve and CD21^{hi} or CD21^{int} IgG^{+} MBCs. Regions are further clustered based on the comparison(s) in which they come out as significant and ordered based on the fold change in accessibility between CD21^{hi} and CD21^{int} IgG^{+} MBCs. Group labels, conditions of inclusion and number of included regions are indicated on the left side of the heatmap. Regions associated with NOTCH regulation of genes belonging to the RYAN_NOTCH_DIRECT geneset (Ryan et al., 2017) are further highlighted on the right side of the heatmap. **(D-G)** Integrative genomic viewer windows for indicated genes showing integrated bulk RNA-seq and ATAC-seq data from all donors for sorted naive and CD21^{hi} or CD21^{int} IgG^{+} MBCs. Identified regions from our bulk-ATAC-seq dataset, annotated Enhancer TSS association (Andersson et al., 2014), ETV6, MYC (ENCODE) and NOTCH (Ryan et al., 2017) binding sites are further displayed in addition for GM 12878 RNAPII ChIA-PET data (Tang et al., 2015) for (E-G). In (D), plots of individual bulk RNA-seq data (normalized counts) and ATAC-seq data (normalized reads) for each sample are also displayed for HES4 and its identified NOTCH target differentially accessible region (Region_11).

Figure S6, related to Figure 5

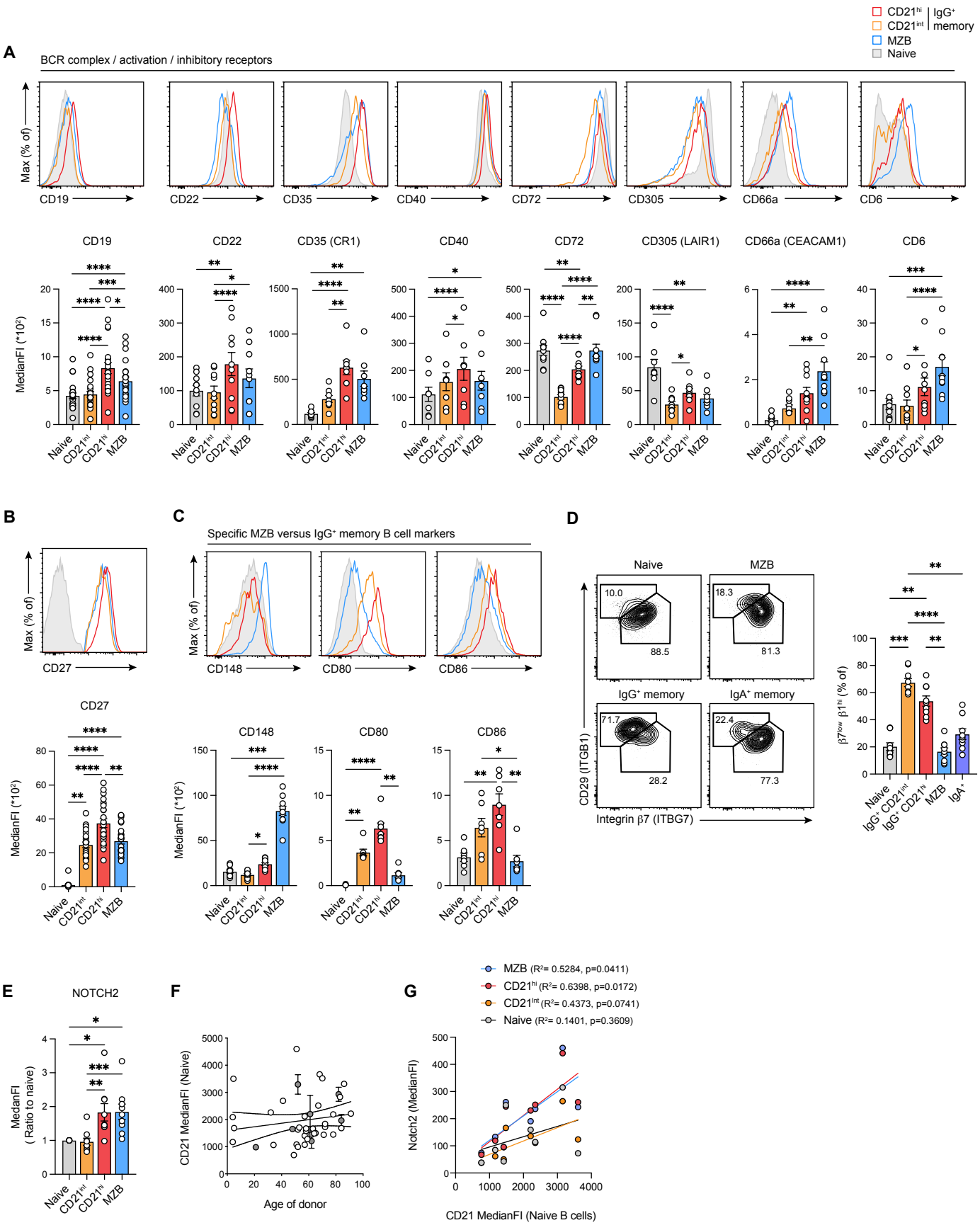

Figure S6. CD21^{hi} IgG^{+} splenic MBCs share partial phenotype and homing potential with splenic marginal zone B cells. Related to Figure 5.

(A) Representative overlayed histograms (top) and graph showing median fluorescence intensities (MedianFI, bottom) for indicated markers in gated splenic naive, CD21^{int} or CD21^{hi} IgG^{+} MBCs (gated as in **Figure 3D**) and IgD^{+}CD27^{+} marginal zone B cells (MZB). For CD22, CD35, CD40, CD72, CD305, CD66a and CD6, corrected median fluorescence intensities are reported, subtracting the intensity values obtained from corresponding isotype control (n = 8-10 HD donors, except CD19: n = 23 HD donors). **(B)** Representative overlayed histograms (top) and graph showing MedianFI for CD27 (bottom, n = 23 HD donors). **(C)** Representative overlayed histograms (top) and graph showing MedianFI for indicated markers (bottom) in gated splenic naive, CD21^{int} or CD21^{hi} IgG^{+} MBCs and IgD^{+}CD27^{+} marginal zone B cells (MZB). For all corrected median fluorescence intensities are reported, subtracting the intensity values obtained from corresponding isotype controls (n = 7-10 HD donors). **(D)** Representative dot plots for integrin β1 (CD29) and integrin β7 staining and gating strategies (left) and graph showing frequencies of integrin β1^{hi} integrin β7^{low} (right) in gated splenic naive, CD21^{int} or CD21^{hi} IgG^{+} MBCs, IgA^{+} MBCs and IgD^{+}CD27^{+} marginal zone B cells (MZB) (n = 9 HD donors). **(E)** Graph showing MedianFI for surface expression of NOTCH2 expressed as a ratio to naive B cell MedianFI from the same donor (n = 9 HD donors). **(F)** Graph showing naive B cells CD21 MedianFI as compared to donor's age (n = 8 HD donors). Linear regression and 95% confidence intervals are shown. **(G)** Graph showing MedianFI for surface expression of NOTCH2 in gated splenic naive, CD21^{int} or CD21^{hi} IgG^{+} MBCs and IgD^{+}CD27^{+} marginal zone B cells (MZB) as compared to naive B cell CD21 MedianFI (n = 8 HD donors). Linear regressions for each population are shown. A non-parametric Friedman test with Benjamini, Krieger and Yekutieli FDR correction was used for all multiple comparisons. Only significant p-values are reported. (****P < 0.0001, ***P < 0.001, **P < 0.01, *P < 0.05).

Figure S7, related to Figure 6

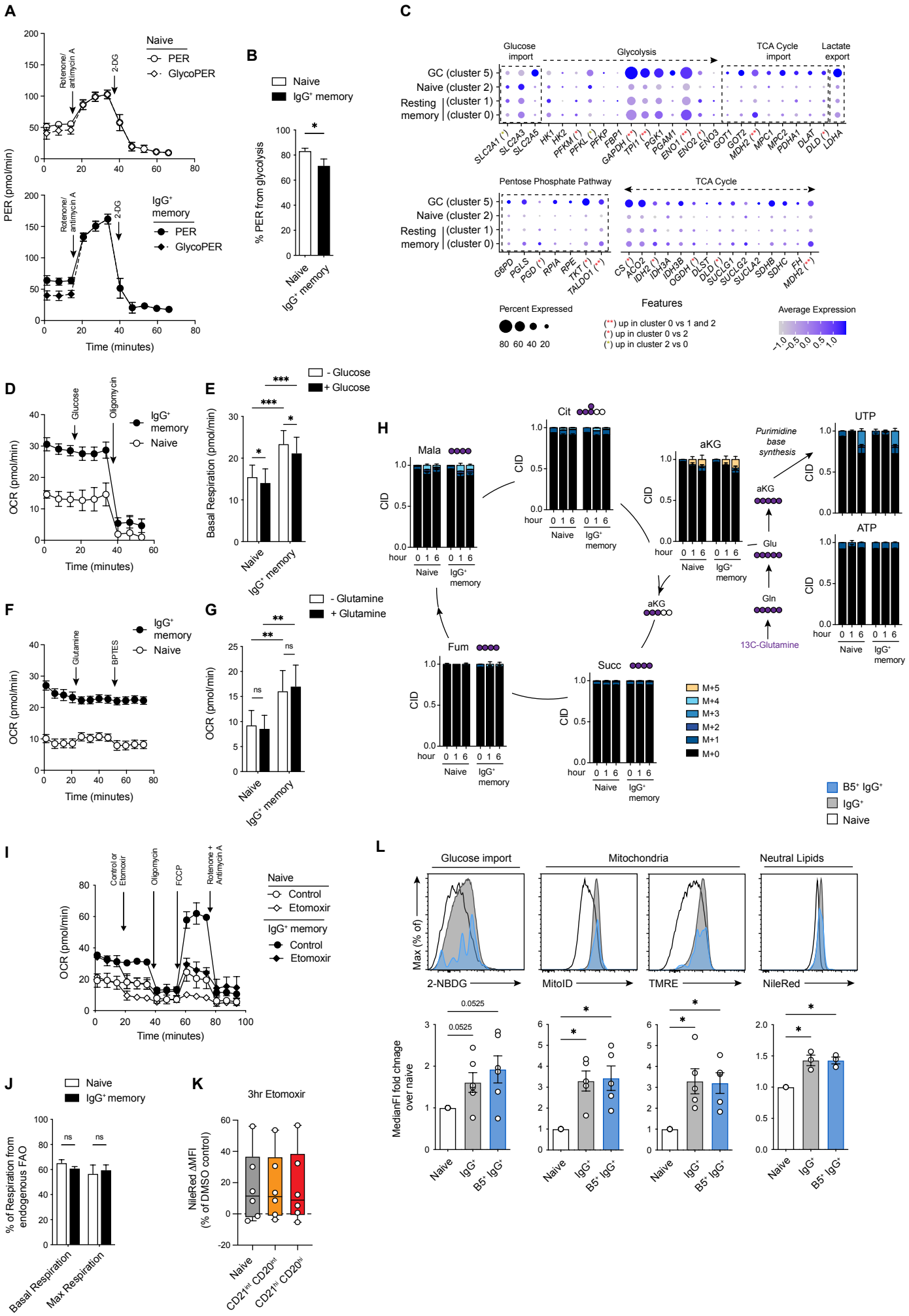

Figure S7. CD21^{hi} IgG^{+} splenic MBCs display enhanced metabolic activity. Related to Figure 6.

(A) Representative Seahorse XF Glycolytic rate assay's proton efflux rate (PER) results and **(B)** calculated PER coming from glycolysis for sorted splenic naive and IgG^{+} MBCs (*n* = 5 HD donors). **(C)** Dot plots showing expression of detected genes coding for proteins involved in glucose import, glycolysis, TCA cycle import, lactate export, the pentose phosphate pathway or the TCA cycle in clusters 0 (CD21^{hi}), 1 (CD21^{int}), 2 (Naives) and 5 (GC) of our scRNA-seq dataset. Size of dots represents the percentage of cells in the cluster in which transcripts for that gene are detected. Dot color represents the average expression (scaled normalized counts) of that gene in the population. Genes significantly differentially expressed in comparisons of interest are further highlighted by asterisks. **(D)** Representative Seahorse XF Gluco stress test's oxygen consumption rate (OCR) results and **(E)** average OCR prior to and after glucose addition for sorted splenic naive and IgG^{+} MBCs (*n* = 5 donors). **(F)** Representative Seahorse XF Glutamine oxidation stress test's OCR results and **(G)** average OCR prior to and after glutamine addition for sorted splenic naïve and IgG^{+} MBCs (*n* = 5 donors). **(H)** Isotopomer distribution in all detected metabolites from splenic naive and total IgG^{+} MBCs at 0, 1 and 6 hours post incubation with labelled ^{13}C-Glutamine (n = 3 HD donors). Color scale represents the number of labeled carbon per metabolite (from none (M+0) to five (M+5)). **(I)** Representative Seahorse XF Mito stress test's OCR results with or without an initial addition of CPT1a inhibitor (etomoxir) and **(J)** calculated basal and maximal respiration coming from endogenous fatty acid oxidation (n = 5 donors). **(K)** Observed changes in NileRed MedianFI, expressed as a percentage of the DMSO control sample, after a 3 hours incubation with etomoxir for naive and CD21^{hi} or CD21^{int} IgG^{+} MBCs (*n* = 6 donors). **(L)** Representative overlayed histograms (top) and graph showing the fold change in TMRE, MitoID and NileRed median fluorescence intensities and 2-NBDG incorporation (bottom) over naive B cells from the same donor for splenic B5^{+}IgG^{+} and total IgG^{+} MBCs (*n* = 3-6 HD donors). (A-M) Mean±SEM. (B) Paired t-test. (E, G, J) Repeated measure two-way and (M) one-way ANOVA. Benjamini, Krieger and Yekutieli FDR correction was used for all multiple comparisons. (***$P < 0.001$, **$P < 0.01$, *$P < 0.05$, n.s. non-significant).